$K^\pi = 8^-$ isomers of the $N = 74$ isotones with the nucleon-pair approximation

Y. Lei,[1,*] G. J. Fu,[2] and Y. M. Zhao[2,†]

[1]*Key Laboratory of Neutron Physics, Institute of Nuclear Physics and Chemistry, China Academy of Engineering Physics, Mianyang 621900, China*

[2]*Physics Department, Shanghai Jiao Tong University, Shanghai, 200240, China*

(Received 14 December 2012; revised manuscript received 21 March 2013; published 25 April 2013)

With the nucleon-pair approximation, we study low-lying structures of three $N = 74$ isotones, ^{128}Xe, ^{130}Ba, and ^{132}Ce, and focus on their $K^\pi = 8^-$ isomers. Negative-parity spin-3$\hbar$ and spin-8$\hbar$ pairs are introduced to construct negative-parity eigenstates. Our calculation well reproduces low-lying energy spectra and the electromagnetic properties of the $K^\pi = 8^-$ isomers. Calculated wave functions of $K^\pi = 8^-$ isomers agree with the previous conjecture, that these isomers are given by a two-quasiparticle excitation, $(\nu\frac{7}{2}^+[404] \otimes \nu\frac{9}{2}^-[514])^{(8)-}$. We discuss the effect of the $\nu g_{7/2}$ single-particle energy evolution on the structure of the $K^\pi = 8^-$ isomer, and predict a similar isomeric mechanism in $N < 73$ even-even isotones. The 3_1^-, 5_1^-, and 7_1^- states of ^{130}Ba and ^{132}Ce are interpreted in terms of octupole vibration or quadrupole-octupole coupling.

DOI: 10.1103/PhysRevC.87.044331 PACS number(s): 21.60.Cs, 23.20.Lv, 23.35.+g, 27.60.+j

I. INTRODUCTION

Isomeric $K^\pi = 8^-$ states have been observed in the even-even $N = 74$ isotones with $Z = 54$–64 [1–6]. Their half-lives range from nanoseconds to milliseconds, with excited energies around 2.5 MeV. Reerences [7–11] suggested that these isomers are given by a two-quasiparticle (2-qp) excitation, $(\nu\frac{7}{2}^+[404] \otimes \nu\frac{9}{2}^-[514])^{(8)-}$. For well deformed $N = 74$ isotones, the $K^\pi = 8^-$ isomer can be explicitly attributed to the K forbiddenness. However, in $N = 74$ isotones with relatively small deformation, the K mixing in low-lying states is enhanced, and the isomeric mechanism is not fully understood.

It would be desirable to study microscopic structures of slightly deformed $K^\pi = 8^-$ isomers by using the shell model [12]. However, the full shell-model space is too gigantic. One can make use of the nucleon-pair approximation (NPA) [13] to truncate the shell-model space. This approach normally considers few positive-parity collective nucleon pairs (e.g., SD pairs with spin 0$\hbar$ and spin 2$\hbar$ [14–18]), which are expectedly able to construct most low-lying configurations. Thus, the NPA could efficiently reproduce the low-lying states, but within a very small model space. However, with only positive-parity pairs, the NPA cannot describe negative-parity states of even-even nuclei. Therefore, the introduction of the negative-parity pair (e.g., the negative-parity dipole P pair [19]) is essential for the NPA study on the $K^\pi = 8^-$ isomer.

In this work, we adopt the NPA with negative-parity pairs to investigate the low-lying energy spectra and the $K^\pi = 8^-$ isomeric electromagnetic properties of three slightly deformed $N = 74$ isotones, i.e., ^{128}Xe, ^{130}Ba, and ^{132}Ce. The resultant NPA wave functions reveal the microscopic structure and isomeric mechanism of the $K^\pi = 8^-$ isomer. We also study the octupole collectivity in some low-lying negative-parity states.

This paper is organized as follows. In Sec. II, we introduce the NPA model space, Hamiltonian, and transition operator. In Sec. III, we present calculated results, including low-lying spectra and electromagnetic properties. We further discuss structures of negative-parity states with resultant NPA wave functions. In Sec. IV, we summarize this work.

II. THE NUCLEON-PAIR APPROXIMATION OF THE SHELL MODEL

A. Configuration space

The NPA model space is constructed with nucleon collective pairs, which is defined as

$$A^{r\dagger} = \sum_{a\leqslant b} \beta^r_{ab} A^{r\dagger}(ab), \quad A^{r\dagger}(ab) = (C^\dagger_a \times C^\dagger_b)^r, \tag{1}$$

where r is the spin of the collective pair; $C^\dagger_a$ represents an operator creating one nucleon in the a orbit; $A^{r\dagger}(ab)$ is a noncollective pair with one nucleon in orbit a and the other in orbit b, and coupled into spin r; β^r_{ab} is the structure coefficient of the collective pair. For $2N$ valence nucleons, the basis in the NPA model space is the successive coupling of N collective pairs,

$$|\tau J_n\rangle = ((A^{r_1\dagger} \times A^{r_2\dagger})^{(J_2)} \times \cdots \times A^{r_N\dagger})^{(J_N)}|0\rangle. \tag{2}$$

In this work, the structure coefficients, β^r_{ab}, are obtained with the following procedure. First, we diagonalize our Hamiltonian in the space $(S^\dagger_{j_1} S^\dagger_{j_2} S^\dagger_{j_3} \cdots)^N$, with $S^\dagger_j = (C^\dagger_j \times C^\dagger_j)^0$, and j running over all the single-particle (s.p.) orbits. β^0_{jj} for the S pair are obtained by maximizing the overlap between the ground state from the above diagonalization and configuration $(S^\dagger)^N$. For β^r_{ab} with spin $r \neq 0$, we diagonalize the same Hamiltonian in the $(S^\dagger)^{N-1}A^{r\dagger}(ab)$ space, with a,b running over all the s.p. orbits. The resultant low-lying wave functions are taken as β^r_{ab}.

In this work, besides conventional positive-parity SD pairs, we also consider two types of negative-parity pairs with spin

*leiyang19850228@gmail.com

†Corresponding author: ymzhao@sjtu.edu.cn

$3\hbar$ and spin $8\hbar$, denoted as F^- and K^- pairs, respectively. Because of computational limit, we only permit one F^- pair in each neutron basis, and one K^- pair in the seniority-2 neutron basis. The F^- pair corresponds to the octupole collectivity, and the K^- pair, we will see, corresponds to the 2-qp excitation in the $K^\pi = 8^-$ isomer.

B. The shell-model Hamiltonian and electromagnetic operator

The shell model Hamiltonian in this work is defined as follows:

$$H = \sum_{\sigma=\pi,\nu} \left\{ \sum_j \varepsilon_{j\sigma} \hat{n}_{j\sigma} - (G_{0\sigma} \mathcal{P}^{0\dagger}_\sigma \cdot \tilde{\mathcal{P}}^0_\sigma + G_{2\sigma} \mathcal{P}^{2\dagger}_\sigma \cdot \tilde{\mathcal{P}}^2_\sigma + \kappa_\sigma Q_\sigma \cdot Q_\sigma) \right\} - \kappa_3 Q^3_\nu \cdot Q^3_\nu + \kappa_{\pi\nu} Q_\pi \cdot Q_\nu, \quad (3)$$

where

$$\mathcal{P}^{0\dagger} = \sum_a \frac{\sqrt{2a+1}}{2} (C^\dagger_a \times C^\dagger_a)^0,$$
$$\mathcal{P}^{2\dagger} = \sum_{ab} q(ab2)(C^\dagger_a \times C^\dagger_b)^2,$$
$$Q = \sum_{ab} q(ab2)(C^\dagger_a \times \tilde{C}_b)^2, \quad (4)$$
$$Q^3 = \sum_{ab} q(ab3)(C^\dagger_a \times \tilde{C}_b)^3,$$
$$q(ab\lambda) = -\sqrt{\frac{2a+1}{2\lambda+1}} \frac{\langle a||r^\lambda Y^\lambda||b\rangle}{r_0^\lambda}.$$

In Eq. (4), r_0 is the oscillator parameter $\sqrt{\frac{\hbar}{m\omega}} \approx 1.012A^{1/3}$ fm; $\varepsilon_{j\sigma}$ corresponds to single-particle (s.p.) energy; $G_{0\sigma}$, $G_{2\sigma}$, κ_σ, κ_3, and $\kappa_{\pi\nu}$ correspond to two-body interaction parameters of the monopole pairing, quadrupole pairing, quadrupole-quadrupole interactions between like nucleons, neutron octupole-octupole interaction, and proton-neutron quadrupole-quadrupole interaction, respectively. Because the valence proton is particle-like, and the valence neutron is hole-like, $\kappa_{\pi\nu}$ is negative. All the Hamiltonian parameters are listed in Table I.

TABLE I. Hamiltonian parameters (MeV). Neutron and proton s.p. energies in the 50–82 shell are taken from Refs. [16,20] and Fig. 1. The s.p. energy of the $g_{9/2}$ orbit from the fpg shell is set as 8 MeV according to the major shell energy. Two-body interaction strengths are adjusted to fit energy levels of low-lying yrast states [20].

	$s_{1/2}$	$d_{3/2}$	$d_{5/2}$	$g_{7/2}$	$h_{11/2}$	$g_{9/2}$
ε_ν	0.331	0.000	1.654	1.350	0.242	8.000
ε_π	2.990	2.439	0.962	0.000	2.791	

	$G_{0\pi}$	$G_{2\pi}$	κ_π	$G_{0\nu}$	$G_{2\nu}$	κ_ν	κ_3	$\kappa_{\pi\nu}$
^{128}Xe	0.134	0.012	0.038	0.088	0.009	0.032	0.013	0.047
^{130}Ba	0.144	0.009	0.032	0.072	0.007	0.021	0.010	0.048
^{132}Ce	0.146	0.007	0.027	0.072	0.006	0.018	0.010	0.043

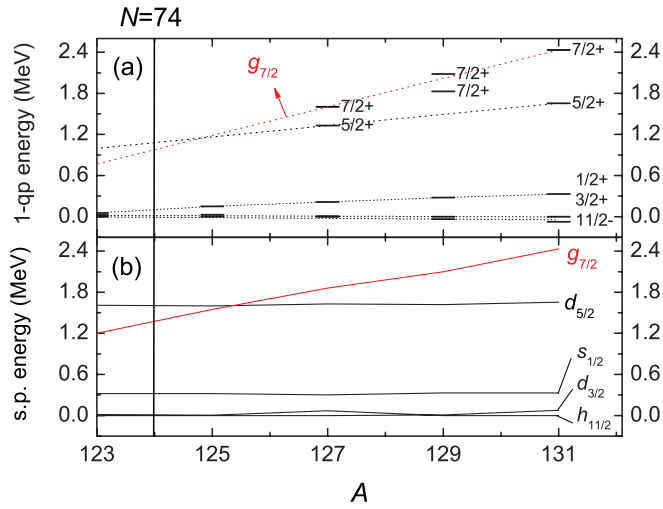

FIG. 1. (Color online) Extraction of neutron s.p. energies from extrapolation of 1-qp energies of the Sn-isotope chain. Panel (a) presents experimentally assigned or systematically supposed 1-qp states from Ref. [20] (all $\nu h_{11/2}$ 1-qp energies are reset as 0 MeV), which are passed through by dotted curves to extrapolate the unknown 1-qp energies. Panel (b) presents the best-fit s.p. energies to extrapolated 1-qp energies in panel (a) within the BCS frameworks as described in Ref. [16]. The red color highlights all the data of the $\nu g_{7/2}$ orbit. The $\nu g_{7/2}$ s.p. energies in this work are taken from the $N = 74$ line.

In the Hamiltonian, the octupole-octupole interaction is included to account for the octupole collectivity of the ^{132}Sn region suggested in Ref. [21]. We also note that the octupole mode always involves the abnormal-parity s.p. orbit, i.e., $h_{11/2}$ orbit in this work, and the $\pi h_{11/2}$ s.p. energy is much higher than the proton Fermi surface in ^{128}Xe, ^{130}Ba, and ^{132}Ce (see Table I). Therefore, the proton octupole mode could be significantly depressed in the low-lying states, and thus we neglect the proton octupole-octupole interaction to save computing time.

In this work, the NPA calculation is mainly performed within the 50–82 shell. Corresponding s.p. energies are taken from s.p. states of ^{133}Sb and ^{131}Sn [20], except those of $\pi s_{1/2}$, $\nu h_{11/2}$ orbits and $\nu g_{7/2}$. $\pi s_{1/2}$ and $\nu h_{11/2}$ energies have not yet been quantitatively measured. Therefore, we take them from Ref. [16]. The $\nu g_{7/2}$ energy in Table I is much different from that in previous NPA calculations [14–18], because it is extracted from the extrapolated 1-qp excited energies of odd-A Sn isotopes. Figure 1(a) presents such an extrapolation, where a series of curves pass through experimentally identified 1-qp levels, and indicate possible excited energies of unknown 1-qp levels. By using the BCS approach[1] as described in Ref. [16], we adjust the s.p. energies to fit the extrapolated 1-qp energies of Fig. 1(a). The resultant s.p. energies are presented in Fig. 1(b), where the $\nu s_{1/2}$, $\nu d_{3/2}$, $\nu d_{5/2}$, and $\nu h_{11/2}$ s.p. energies are very stable. Therefore, this work safely adopts the

[1]In the BCS framework, 1-qp excited energy is given by $E_i = \sqrt{(e_i - \lambda)^2 + \Delta^2}$, where e_i, λ, and Δ correspond to s.p. energy, chemical potential, and pair gap, respectively.

excited energies of s.p. states in ^{131}Sn as the s.p. energies of corresponding orbits in $N = 74$ isotones. However, the $\nu g_{7/2}$ s.p. energy is obviously depressed with increasing valence neutron number. This work takes the $\nu g_{7/2}$ s.p. energy from the $N = 74$ extrapolation in Fig. 1(b) as 1.350 MeV.

We emphasize that the depression of the $\nu g_{7/2}$ s.p. energy has little effect on low-lying yrast states, because the $\nu g_{7/2}$ s.p. energy is always higher than the neutron Fermi surface for $N > 73$ nuclei as shown in Fig. 1(b). That is why few previous works considered it. However, it essentially affects the structure of the $K^\pi = 8^-$ isomer, which we will demonstrate in Sec. III B.

Additionally, we introduce the $\nu g_{9/2}$ orbit into our s.p. space for two reasons. First, the Nilsson state, $\frac{7}{2}^+[404]$, is a linear combination of $g_{7/2}$ and $g_{9/2}$ orbits; $(\nu\frac{7}{2}^+[404] \otimes \nu\frac{9}{2}^-[514])^{(8)-}$ is expected to be the main component of the $K^\pi = 8^-$ isomer. Therefore, the neutron $g_{9/2}$ orbit is essential to construct such an isomer. Second, in $N = 74$ isotones, there are systematic $E1$ transitions from $K^\pi = 8^-$ isomers to yrast 8^+ states; however, no $E1$ transition can exist within the 50–82 shell. The $g_{9/2}$ degree of freedom is a possible solution for this "no $E1$" problem.

The s.p. energy of the $g_{9/2}$ orbit is estimated as 8 MeV according to the major shell energy, $\hbar\omega = 41/A^{1/3} \sim 8$ MeV, which is much higher than those in the 50–82 shell. Thus, the $g_{9/2}$ s.p. energy has very little effect on low-lying states. For example, according to our trial calculation, it only produces ~10 keV binding-energy difference and a difference of $B(E1, 8_1^- \to 8_1^+)$ in two orders of magnitude as the $g_{9/2}$ s.p. energy varies from 3 to 20 MeV. It could be safely taken as 8 MeV without delicate adjustment.

The electromagnetic transition operator is given by

$$T(EL) = \sum_i e_i r_i^L Y^L,$$

$$T(ML) = \sqrt{L(2L+1)} \sum_i r_i^{L-1} \left\{ \frac{2g_{li}}{L+1} [Y^{L-1} \times \vec{l}\,]^L + 2g_{si}[Y^{L-1} \times \vec{\sigma}\,]^L \right\}, \quad (5)$$

where e_i, g_{li}, and g_{si} are the effective charge, orbital gyromagnetic ratio, and spin gyromagnetic ratio of the ith valence nucleon, respectively. The magnetic momentum is defined by

$$\mu = \langle IM = I | \sqrt{\frac{4\pi}{3}} T(M1) | IM = I \rangle. \quad (6)$$

III. RESULTS AND ANALYSIS

A. Spectra and electromagnetic properties

Figure 2 presents the calculated energy levels of ^{128}Xe, ^{130}Ba, and ^{132}Ce, and compares them with experimental spectra. The NPA calculation reasonably reproduces low-lying yrast states. The calculated 8_1^- states of these nuclei are all very close to the experimental $K^\pi = 8^-$-isomer levels. Other negative-parity energy levels are also roughly consistent with experimental levels, except that calculated 6_1^- and 7_1^- levels of ^{128}Xe are much higher than experimental ones.

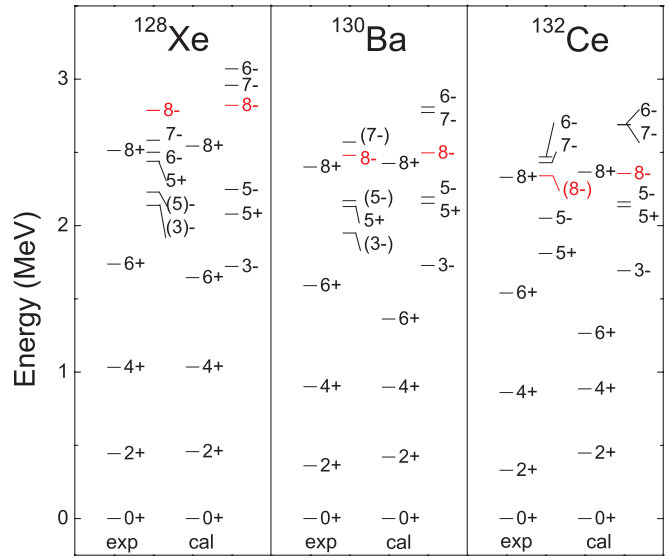

FIG. 2. (Color online) Low-lying levels of ^{128}Xe, ^{130}Ba, and ^{132}Ce. The experimental data [20] and calculated spectra are denoted by "exp" and "cal", respectively. The $K^\pi = 8^-$ isomer is highlighted with the red level.

Table II lists the calculated electromagnetic transitions, magnetic moments, and half-lives of $K^\pi = 8^-$ isomers for ^{128}Xe, ^{130}Ba, and ^{132}Ce, as well as corresponding experimental data. For the $E2$ and $E3$ transition, the effective charges are adjusted to fit to $E2$ transition rates between yrast states assuming $e_\pi = -e_\nu$ [15–17,22]. The resultant effective charges are $e_\pi = -e_\nu = 2.1e$. The calculated yrast $E2$ transitions are consistent with experimental ones (see the first four rows in Table II), which indicates that these effective charges are reasonable. The neutron effective charge for the $E1$ transition is set as $-3Z/(10A)e$ [23] considering the center mass motion. We do not consider proton $E1$ effective charge, because the valence proton does not contribute to the $E1$ transition in our calculation framework. The gyromagnetic ratios are directly taken from the χ^2 fitting of effective g factor in Ref. [18]; they are $g_{l\pi} = 1\mu_N$, $g_{l\nu} = 0.044\mu_N$, $g_{s\pi} = 5.586 \times 0.7\mu_N$, and $g_{s\nu} = -3.826 \times 0.7\mu_N$.

As shown in Table II, the calculated magnetic moment of the $K^\pi = 8^-$ isomer in ^{128}Xe is consistent with the experimental data within error, which was the very clue to propose the $(g_{7/2} \otimes h_{11/2})^{(8)}$ configuration [7], i.e., $(\frac{7}{2}^+[404] \otimes \frac{9}{2}^-[514])^{(8)-}$ with slight deformation. This agreement on magnetic moment hints that our resultant wave function of the $K^\pi = 8^-$ isomer in ^{128}Xe may also correspond to the $(\frac{7}{2}^+[404] \otimes \frac{9}{2}^-[514])^{(8)-}$ configuration. We also present calculated magnetic moments of ^{132}Ba and ^{132}Ce, which may deserve further experimental examination.

Because 8_1^- states are supposed isomers, all decay strengths from 8_1^- states shall be very weak. Calculated transition rates from 8_1^- states indeed are smaller than 10^{-1} W.u. Moreover, the orders of calculated transition rates are also reasonably consistent with experimental data. Typically, calculated $B(E1, 8_1^- \to 8_1^+)$'s with order of 10^{-11} W.u. agree with the experimental order of 10^{-12}–10^{-11} W.u. Introduction of the

TABLE II. Electromagnetic transitions (W.u.), 8_1^- magnetic moments (μ_N), and half-lives ($\tau_{1/2}$) in $N = 74$ isotones. All experimental data are from Ref. [20]. The $E2/E3$ effective charges and gyromagnetic ratios are set as $e_\pi = 2.1e$, $g_{l\pi} = 1\mu_N$, and $g_{s\pi} = 5.586 \times 0.7\mu_N$; $e_\nu = -2.1e$, $g_{l\nu} = 0.044\mu_N$, and $g_{s\nu} = -3.826 \times 0.7\mu_N$. The neutron $E1$ effective charge are set as $-3Z/(10A)e$. "> 0" in this table means corresponding electromagnetic transition has been observed but its transition rate have not been measured quantitatively yet. The decay rates labeled "*" correspond to the main branch of the $K^\pi = 8^-$ isomer decay.

	^{128}Xe		^{130}Ba		^{132}Ce	
	Expt.	Calc.	Expt.	Calc.	Expt.	Calc.
$B(E2, 2_1^+ \to 0_1^+)$	40.2(21)	50.0	57.9(17)	47.6	93(7)	78.2
$B(E2, 4_1^+ \to 2_1^+)$	59(5)	57.6	78.9(13)	52.2	103(23)	83.6
$B(E2, 6_1^+ \to 4_1^+)$	78(7)	82.4	94(6)	67.4	140(80)	102
$B(E2, 8_1^+ \to 6_1^+)$	96(11)	59.4	9(3) × 10	59.7	68(14)	39.3
$\mu(8_1^-)$	−0.29(7)	−0.31		−0.19		−0.18
$B(E1, 8_1^- \to 8_1^+)$		5.7×10^{-11}	$4.0(5) \times 10^{-12}$	2.9×10^{-11}	$2.2(9) \times 10^{-11}$	3.3×10^{-11}
$B(E2, 8_1^- \to 6_1^-)$	$4.7(9) \times 10^{-2}$	1.5×10^{-2}*		2.6×10^{-2}		2.9×10^{-2}
$B(E3, 8_1^- \to 6_1^+)$		6.6×10^{-4}	$1.3(7) \times 10^{-4}$	8.8×10^{-4}		1.3×10^{-3}*
$B(M1, 8_1^- \to 7_1^-)$	$1.5(5) \times 10^{-5}$	9.8×10^{-6}		1.4×10^{-5}		1.1×10^{-5}
$B(M2, 8_1^- \to 6_1^+)$		8.9×10^{-5}	$8(5) \times 10^{-8}$	1.1×10^{-5}*	$2.6(4) \times 10^{-7}$	1.3×10^{-6}*
$\tau_{1/2}(8_1^-)$	82(3) ns	553 ns	9.4(4) ms	0.4 ms	9.3(3) ms	4.1 ms
$B(E3, 3_1^- \to 0_1^+)$		63		58		61
$B(E2, 5_1^- \to 3_1^-)$		94		82		69
$B(E2, 7_1^- \to 5_1^-)$		74	110(7)	84		79

$g_{9/2}$ orbit indeed well reproduces the weak $E1$ transition from the $K^\pi = 8^-$ isomer. Based on these small calculated transition strengths, we also calculate half-lives of $K^\pi = 8^-$ isomers, which are all consistent with experimental ones as shown in Table II.

Experiments have observed $E2$ transitions between 5_1^- and 7_1^- states in all three $N = 74$ isotones [20]; the $B(E2, 7_1^- \to 5_1^-)$ of ^{130}Ba was even quantitatively measured as 110(7) W.u. Our calculation also gives a large $B(E2, 7_1^- \to 5_1^-) \sim 80$ W.u. for all three isotones. Additionally, a series of strong $E2/E3$ transitions are also obtained between the ground state, 3_1^-, and 5_1^- states. Empirically, such strong $E2/E3$ transitions demonstrate quadrupole/octupole correlations, which implies octupole vibration [21] or quadrupole-octupole coupling [24] in these negative-parity states.

B. Wave function and analysis

Table III presents expectation numbers of non-S pairs in calculated eigenstates to indicates which and how many non-S pairs are involved in corresponding eigenstates. We do not present the S pair number, because it can be readily obtained according to total-pair-number conservation.

According to Table III, the $K^\pi = 8^-$ isomers in all three $N = 74$ isotones mainly correspond to a 2-qp configuration with the K^- pair excitation. On the other hand, the 6_1^+, 8_1^+, 7_1^-, and 6_1^- states all correspond to 6-qp or 8-qp excitations. Empirically, they cannot have large electromagnetic transition matrix elements with a 2-qp configuration, i.e., the $K^\pi = 8^-$ isomer in this work, because the transition operator usually could only excite one 2-qp configuration or just scatter an existing 2-qp configuration into another one (i.e., the operator could only change the number of quasiparticles by 2). That is why the decay strengths from $K^\pi = 8^-$ isomers to these states are so weak.

Table III also demonstrates calculated 3_1^-, 5_1^-, and 7_1^- states are mainly constructed with D pairs and one F^- pair, which imply the quadrupole and octupole collectivities, respectively. This observation agrees with the octupole-vibration or quadrupole-octupole-coupling picture, which is also suggested by strong $E2/E3$ decay rates from these states in Sec. III A. However, as shown in Fig. 2, calculated 6_1^- and 7_1^- states of ^{128}Xe are higher than experimental ones, which indicates that the quadrupole-octupole coupling picture does not work for ^{128}Xe. One may need more types of negative-parity pairs to interpret these states.

Previous experiments assigned the $K^\pi = 8^-$ isomer as the $(\frac{7}{2}^+[404] \otimes \frac{9}{2}^-[514])^{(8)-}$ configuration; on the other hand, the $K^\pi = 8^-$ isomer obtained from our calculation corresponds

TABLE III. Expectation numbers of D, F^-, and K^- pairs in calculated eigenstates. Some pair numbers are not listed in this table if they are smaller than 0.0005.

State	Pair	^{128}Xe	^{130}Ba	^{132}Ce
8_1^-	D	0.073	0.036	0.125
	K^-	1.000	1.000	1.000
6_1^+	D	2.951	3.013	3.112
8_1^+	D	4.099	4.285	4.357
6_1^-	D	2.020	2.029	2.119
	F^-	1.000	1.000	1.000
3_1^-	D^-	0.053	0.046	0.088
	F^-	1.000	1.000	1.000
5_1^-	D	1.007	1.054	1.160
	F^-	1.000	1.000	1.000
7_1^-	D	1.951	2.005	2.107
	F^-	1.000	1.000	1.000

TABLE IV. Single-particle occupation numbers of 2-qp configurations for the $K^\pi = 8^-$ isomer. The occupation in the $(\frac{7}{2}^+[404] \otimes \frac{9}{2}^-[514])^{(8)-}$ configuration is obtained according to the Nilsson scheme. In the corresponding Nilsson Hamiltonian, the deformation parameters are taken from Ref. [25] ($\varepsilon_2 = 0.133, 0.158, 0.183$; $\varepsilon_4 = 0.000, 0.013, 0.027$ for ^{128}Xe, ^{130}Ba, ^{132}Ce, respectively); other parameters are from Eq. (8.5) of Ref. [26] ($\kappa = 0.0637$ and $\mu = 0.42$). We list two sets of K^--pair s.p. occupations for both $N = 74$ and $N = 76$ cases. The $N = 74$ K^- pair corresponds to the K^- pair used in this work. The $N = 76$ K^- pair is obtained with $\nu g_{7/2}$ s.p. energy (= 1.75 MeV) from the $N = 76$ extrapolation in Fig. 1(b). The two-body interaction strengths for the $N = 76$ K^- pair are the same as those for $N = 74$. "$< 10^{-2}$" in this table means the corresponding occupation number is smaller than 0.005.

	^{128}Xe				^{130}Ba				^{132}Ce			
	$h_{11/2}$	$g_{9/2}$	$g_{7/2}$	$d_{5/2}$	$h_{11/2}$	$g_{9/2}$	$g_{7/2}$	$d_{5/2}$	$h_{11/2}$	$g_{9/2}$	$g_{7/2}$	$d_{5/2}$
$(\frac{7}{2}^+[404] \otimes \frac{9}{2}^-[514])^{(8)-}$	1.00	$<10^{-2}$	1.00		1.00	$<10^{-2}$	0.99		1.00	$<10^{-2}$	0.99	
K^- for $N = 74$	1.00	$<10^{-2}$	0.89	0.11	1.00	$<10^{-2}$	0.94	0.06	1.00	$<10^{-2}$	0.95	0.05
K^- for $N = 76$	1.00	$<10^{-2}$	0.22	0.78	1.00	$<10^{-2}$	0.23	0.77	1.00	$<10^{-2}$	0.29	0.71

to the K^--pair excitation as shown in Table III. We shall verify whether the structure of the K^- pair is similar to that of $(\frac{7}{2}^+[404] \otimes \frac{9}{2}^-[514])^{(8)-}$ by comparing their s.p. occupation numbers. In Table IV, we list three sets of s.p. occupation numbers: $(\frac{7}{2}^+[404] \otimes \frac{9}{2}^-[514])^{(8)-}$ configuration, $N = 74$, and $N = 76$ K^- pairs. The $N = 74$ K^- pair corresponds to the K^- pair used in this work; the $N = 76$ K^- pair is obtained with the $\nu g_{7/2}$ s.p. energy (= 1.75 MeV) from the $N = 76$ extrapolation in Fig. 1(b).

According to Table IV, $(\frac{7}{2}^+[404] \otimes \frac{9}{2}^-[514])^{(8)-}$ and the $N = 74$ K^- pair have similar occupations: they both have most of two neutrons to occupy $\nu h_{11/2}$ and $\nu g_{7/2}$ orbits, and leave a minute amount on the $\nu g_{9/2}$ orbit. From this perspective, our calculation supports the experimental conjecture on the $K^\pi = 8^-$ isomer; i.e., the $(\frac{7}{2}^+[404] \otimes \frac{9}{2}^-[514])^{(8)-}$ configuration.

In Table IV, the s.p. occupation of the $N = 76$ K^- pair is presented to demonstrate the effect of the $\nu g_{7/2}$ s.p. energy evolution on the structure of the $K^\pi = 8^-$ isomer. One can see that occupations of $\nu d_{5/2}$ and $\nu g_{7/2}$ orbits in the $N = 76$ K^- pair are very different from those in $(\frac{7}{2}^+[404] \otimes \frac{9}{2}^-[514])^{(8)-}$ and the $N = 74$ K^- pair: the $N = 76$ K^- pair has almost one neutron at the $\nu d_{5/2}$ orbit; while $(\frac{7}{2}^+[404] \otimes \frac{9}{2}^-[514])^{(8)-}$ and the $N = 74$ K^- pair, on the contrary, shift this one neutron to the $\nu g_{7/2}$ orbit. This difference is due to the depression of the $\nu g_{7/2}$ s.p. energy as shown in Fig. 1(b): for $N > 75$, the $\nu d_{5/2}$ s.p. energy is lower than the $\nu g_{7/2}$ one, and thus the $\nu d_{5/2}$ orbit is more occupied; for $N < 75$, the $\nu g_{7/2}$ s.p. energy (i.e., the $\frac{7}{2}^+[404]$ s.p. energy with small deformation) is depressed below $\nu d_{5/2}$, which naturally leads to the $(\frac{7}{2}^+[404] \otimes \frac{9}{2}^-[514])^{(8)-}$ configuration. Because the $\nu g_{7/2}$ s.p. energy in $N < 73$ even-even isotones may be further depressed according to Fig. 1(b), a similar $K^\pi = 8^-$ isomer may also exist in these isotones. For example, the 8^- state of ^{126}Xe ($N = 72$) with 1.3(2) ns half-life and 2758.21(11) keV excited energy [20] could be a candidate.

IV. SUMMARY

In this work, we perform the NPA calculation with negative-parity pairs to study the low-lying states in three $N = 74$ isotones, ^{128}Xe, ^{130}Ba, and ^{132}Ce, to investigate the microscopic structures of their $K^\pi = 8^-$ isomers. Conventional SD pairs and two negative-parity pairs, F^- and K^- pairs, are considered to construct the NPA model space. A shell-model phenomenological Hamiltonian is adopted, including the s.p. energy, monopole pairing, quadrupole pairing, quadrupole-quadrupole interactions, and neutron octupole quadrupole, where the $\nu g_{7/2}$ s.p. energy is extracted from 1-qp excited energies of the Sn isotopes within the BCS framework. The NPA calculation well reproduces low-lying spectra and the $K^\pi = 8^-$ isomeric electromagnetic properties of these $N = 74$ isotones, which demonstrates our calculation is reliable.

According to the expectation pair numbers of resultant eigenstates, the $K^\pi = 8^-$ isomer indeed corresponds to a 2-qp excitation, as most previous experiments assigned; on the other hand, all the states linked to the $K^\pi = 8^-$ isomer by electromagnetic transitions are identified as 6-qp or 8-qp excitations. The large configuration difference between these states and the $K^\pi = 8^-$ isomer leads to weak decay strengths, namely the isomeric observation.

According to the comparison between s.p. occupations of the $K^\pi = 8^-$ 2-qp configurations from NPA calculation and those of the $(\frac{7}{2}^+[404] \otimes \frac{9}{2}^-[514])^{(8)-}$ configurations from the Nilsson scheme, the calculated 2-qp configuration of the $K^\pi = 8^-$ isomer is very similar to the $(\frac{7}{2}^+[404] \otimes \frac{9}{2}^-[514])^{(8)-}$ configuration, which supports pervious experimental conjecture. We also find the $\nu g_{7/2}$ single-particle level evolution has a dominant effect on such a 2-qp structure, according to which we suggest that a similar $K^\pi = 8^-$ isomer might also exist in $N < 73$ even-even isotones.

We also note that the 3_1^-, 5_1^-, and 7_1^- states in ^{130}Ba and ^{132}Ca are mainly constructed by D pairs and one F^- pair. Thus, these states correspond to a typical octupole vibration or quadrupole-octupole coupling. However, we still cannot well describe the 7_1^- state in ^{128}Xe with only D and F^- pairs.

ACKNOWLEDGMENTS

Discussions with Prof. R. F. Casten and Dr. F. Q. Chen are gratefully acknowledged. We thank the anonymous referee for his/her constructive advice. We also thank the National Natural Science Foundation of China for supporting this work under Grants No. 10975096, No. 11145005, and No. 91126001.

[1] H. F. Brinkman, C. Heiser, K. F. Alexander, W. Neubert, and H. Rotter, Nucl. Phys. **81**, 233 (1966).
[2] D. Ward, R. M. Diamond, and F. S. Stephens, Nucl. Phys. A **117**, 309 (1968).
[3] D. G. Parkinson, I. A. Fraser, J. C. Lisle, and J. C. Willmott, Nucl. Phys. A **194**, 443 (1972).
[4] L. Goettig, Ch. Droste, A. Dygo, T. Morek, J. Srebrny, R. Broda, J. Styczèn, J. Hattula, H. Helppi, and M. Jääskeläinen, Nucl. Phys. A **357**, 109 (1981).
[5] A. M. Bruce, P. M. Walker, P. H. Regan, G. D. Dracoulis, A. P. Byrne, T. Kibèdi, G. J. Lane, and K. C. Yeung, Phys. Rev. C **50**, 480 (1994).
[6] A. M. Bruce, A. P. Byrne, G. D. Dracoulis, W. Gelletly, T. Kibèdi, F. G. Kondev, C. S. Purry, P. H. Regan, C. Thwaites, and P. M. Walker, Phys. Rev. C **55**, 620 (1997).
[7] T. Lönnroth, S. Vajda, O. C. Kistner, and M. H. Rafailovich, Z. Phys. A **317**, 215 (1984).
[8] H. Rotter, K. F. Alexander, Ch. Droste, T. Morek, W. Neubert, and S. Chojnacki, Nucl. Phys. A **133**, 648 (1969).
[9] T. Morek, J. Srebrny, Ch. Droste, M. Kowalczyk, T. Rząca-Urban, K. Starosta, W. Urban, R. Kaczarowski, E. Ruchowska, M. Kisieliński, A. Kordyasz, J. Kownacki, M. Palacz, E. Wesołowski, W. Gast, R. M. Lieder, P. Bednarczyk, J. Męczyński, and J. Styczeń, Phys. Rev. C **63**, 034302 (2001).
[10] C. M. Petrache, Y. Sun, D. Bazzacco, S. Lunardi, C. Rossi Alvarez, G. Falconi, R. Venturelli, G. Maron, D. R. Napoli, Zs. Podolyak, and P. M. Walker, Nucl. Phys. A **617**, 249 (1997).
[11] P. H. Regan, G. D. Dracoulis, A. P. Byrne, G. J. Lane, T. Kibédi, P. M. Walker, and A. M. Bruce, Phys. Rev. C **51**, 1745 (1995).
[12] M. G. Mayer, Phys. Rev. **75**, 1969 (1949); J. H. D. Jensen, H. Suess, and O. Haxel, Naturwissenschaften **36**, 155 (1949).
[13] J. Q. Chen, Nucl. Phys. A **626**, 686 (1997); Y. M. Zhao, N. Yoshinaga, S. Yamaji, J. Q. Chen, and A. Arima, Phys. Rev. C **62**, 014304 (2000).
[14] Y. A. Luo and J. Q. Chen, Phys. Rev. C **58**, 589 (1998).
[15] Y. A. Luo, J. Q. Chen, and J. P. Draayer, Nucl. Phys. A **669**, 101 (2000).
[16] Y. M. Zhao, S. Yamaji, N. Yoshinaga, and A. Arima, Phys. Rev. C **62**, 014315 (2000).
[17] K. Higashiyama, N. Yoshinaga, and K. Tanabe, Phys. Rev. C **67**, 044305 (2003).
[18] L. Y. Jia, H. Zhang, and Y. M. Zhao, Phys. Rev. C **76**, 054305 (2007).
[19] F. Catara, M. Sambataro, A. Insolia, and A. Vitturi, Phys. Lett. B **180**, 1 (1986).
[20] Evaluated Nuclear Structure Data, http://www.nndc.bnl.gov/ensdf/.
[21] J. P. Omtvedt, H. Mach, B. Fogelberg, D. Jerrestam, M. Hellström, L. Spanier, K. I. Erokhina, and V. I. Isakov, Phys. Rev. Lett. **75**, 3090 (1995); R. Kshetri, M. S. Sarkar, and S. Sarkar, Phys. Rev. C **74**, 034314 (2006).
[22] S. Raman, C. W. Nestor, Jr., and K. H. Bhatt, Phys. Rev. C **37**, 805 (1988).
[23] I. Hamamoto, Nucl. Phys. A **205**, 225 (1973).
[24] D. R. Haenni and T. T. Sugihara, Phys. Rev. C **16**, 120 (1977); D. R. Zolnowski, T. Kishimoto, Y. Gono, and T. T. Sugihara, Phys. Lett. B **55**, 453 (1975); M. Nomura, *ibid.* **55**, 357 (1975).
[25] P. Möller, J. R. Nix, W. D. Myers, and W. J. Swiatecki, At. Data Nucl. Data Tables **59**, 185 (1995).
[26] R. F. Casten, *Nuclear Structure from a Simple Perspective* (Oxford University Press, Oxford, 2000).